



NOISE CONTROL FOR QUALITY OF LIFE

Initial results for traffic noise mitigation with Helmholtz resonators in the ground surface beside a road

Jens Forssén and Bart van der Aa¹

¹ Department of Civil and Environmental Engineering, Division of Applied Acoustics,
Chalmers University of Technology, SE-41296 Göteborg, Sweden.

ABSTRACT

For reduction of road traffic noise, measures focussing on the propagation path are needed as complements to measures at source. Here, the effect of Helmholtz resonators, buried in the ground surface alongside the road, is investigated. Possible benefits of buried resonators are that they can function without obstructing the accessibility to the protected area. A modelling approach using equivalent sources is described for a coupled field of resonators in an otherwise acoustically hard ground plane. The model is validated in comparison with laboratory measurements. For selected road traffic cases, the model is used to predict the effect of resonators in a grid pattern within a strip along the road, showing noise reductions of 2–4 dBA.

Keywords: Traffic Noise Abatement, Sound Propagation Calculation, Helmholtz Resonators

1. INTRODUCTION

Noise pollution is a major environmental problem. The social costs of traffic noise have been estimated to 0.4 % of total GDP for the European Union, and the main contribution is from roads. At the same time road traffic is expected to steadily increase, the source strength is not expected to significantly decrease within the near future and urbanization is an ongoing process, whereby the reduction of outdoor traffic noise in urban areas is a major issue of high need.

In urban areas acoustic measures like noise barriers are often not wanted and it is seldom possible to achieve significant effects by calming or rerouting traffic. Therefore, the effect of installing resonators in the ground surface alongside the road has been investigated, as one of many alternative approaches to noise reduction during propagation. A benefit of using buried resonators is that they can be made to work without impairing the access to the surface, i.e. pedestrians and cyclists may pass across surfaces with buried resonators.

¹ jens.forssen@chalmers.se

2. METHOD

2.1 Basic principles of Helmholtz resonators

A single Helmholtz resonator basically consists of a closed volume, V_b , which is connected to a neck with a smaller opening area, S_n , see Figure 1. The top neck-opening works as a port through which the resonator communicates with the external medium, here assumed to be a homogeneous atmosphere. A plug of air enclosed in the neck of the resonator will move downwards after a positive pressure pulse is impinging on the resonator opening and will increase the pressure inside the resonator volume. It is, however, important to realize that the resonators neck is small with respect to the acoustic wavelength of interest, both in length and width. Hence the neck particle velocity along the neck can be assumed to be constant. Also the body dimensions are assumed small in comparison with the wavelength.

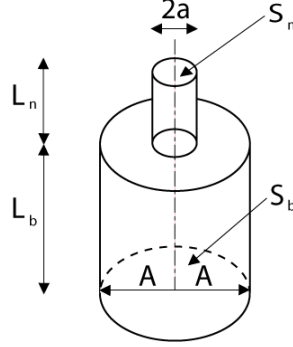


Figure 1 – Representation of a single cylindrical Helmholtz resonator. Here, L_n is the uncorrected length of the neck, L_b the length of the body, A the radius of the body, a the radius of the neck opening, S_n the opening surface area and S_b the surface area of body top and bottom.

A Helmholtz resonator is a simple mass-spring-system where the air in the neck represents the mass and the enclosed air in the volume represents the spring. To calculate the resonance frequency correctly it is necessary to add the mass of the air directly connected at both ends of the neck to the oscillating mass of air in the neck. The resonance frequency f_r of a Helmholtz resonator can then be estimated as

$$f_r = \frac{c}{2\pi} \sqrt{\frac{S_n}{V_b \cdot (L_n + L_{corr})}} \quad (1)$$

Where c is the sound speed and L_{corr} is the correction for the connected air at both ends of the neck. The neck-correction is well described in literature (e.g. [1]) for different shapes of the neck and geometrical setups, for instance for a single circular opening (dating back to Rayleigh): $L_{corr} \approx 8a/(3\pi)$. The formula can be used for the outer end-correction, whereas here we have included an inner end-correction with a slightly smaller size, according to Ingard [1], as:

$$L_{corr,inner} \approx \frac{8a}{3\pi} \left(1 - 1.25 \frac{a}{A} \right). \quad (2)$$

To calculate the impedance of a Helmholtz resonator the approach by Rayleigh is useful, where an incoming pressure eventually results in a velocity of the piston, i.e. the air of the neck. The piston velocity, which is dependent on the resonator characteristics, can be seen as the speed at which the opening surface S_n moves due to an incoming pressure. The impedance of the resonating absorber is constituted by its mass, spring-stiffness and resistance. Using a lumped element model makes it possible to visualize the working system by the mass, spring and resistance elements, see Figure 2.

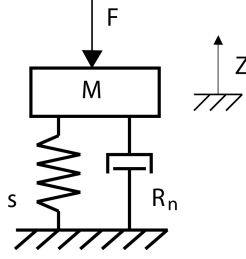


Figure 2 – Lumped element model of a Helmholtz resonator excited by a force, F . Furthermore, M represents the total mass $M_n + M_b$, where M_n is the neck-mass and M_b the correction in connection to the body volume, s is the spring stiffness and R_n the resistance in the neck.

As displayed in Figure 2, the upward displacement is defined as positive and the force, F , is defined in the opposite direction. A force balance results in

$$-F = M a + R_n v + s z. \quad (3)$$

The partial differential equation (Eq. 3) is solved using a frequency domain approach, with $v = j\omega z$ and $a = j\omega v$, where $\omega = 2\pi f$. The impedance, Z , relating pressure and velocity at a common point, can here be written $Z = -p/v$. Using $p = F/S_n$ finally gives the impedance as

$$Z_{hr} = \frac{-F}{S_n v} = \frac{j\omega M + R_n - \frac{j}{\omega} s}{S_n} \quad (4)$$

which links back to the equation for the resonance frequency (Eq. 1) by setting the imaginary part of the impedance equal to zero and using

$$s = \frac{\rho c^2 S_n^2}{V} \quad (5)$$

where ρ is the density of air. The resistance is taken as

$$R_n = \frac{\sqrt{2\rho\omega\mu_0}}{\pi a^2} \left(2 + \frac{L_n}{a} \right) \quad (6)$$

where, μ_0 is the dynamical viscosity of air [1]. The correction used here for the mass connected to the finite size body is, adapted from [2]:

$$M_b = \frac{L_b S_n^2 \rho}{3S_b}. \quad (7)$$

2.2 Prediction model

A model has been developed, where the radiation from the openings of the resonators are modeled as auxiliary monopole point sources in an acoustically hard plane. For an original omnidirectional point source, simulating, one at a time, the different vehicle sources, the sound field can be calculated in any point above the plane, after first determining the source strengths of the auxiliary sources, as is briefly described below.

For a set of N resonators, an equation system needs to be set up and solved. With \mathbf{A} being a matrix of size $N \times N$, \mathbf{q} a vector of length N of the unknown source strengths, q_i , and \mathbf{p} a vector of length N of the incoming pressure from the original source to each resonator opening, the equation system can be written as

$$\mathbf{A} \times \mathbf{q} = \mathbf{p} \quad (8)$$

where elements a_{ij} of \mathbf{A} contain the transfer functions from resonator i to resonator j . Gaussian elimination can be used to solve the equation system, resulting in the resonator amplitudes \mathbf{q} , which are used to calculate the total pressure at the receiver as

$$p(x, y, z) = q [G(r_d) + G(r_r)] + \sum_{i=1}^N q_i G(r_i) \quad (9)$$

where q is the strength of the original source, $G(r)$ is the Green function for a point source in a three-dimensional unbounded space, r_d and r_r are the direct and the ground reflected path lengths from the original source to the receiver and r_i is the distance from resonator i to the receiver. The insertion loss at a certain frequency is then calculated as

$$IL = 20 \log_{10} \left| \frac{q[G(r_d) + G(r_r)]}{q[G(r_d) + G(r_r)] + \sum_{i=1}^N q_i G(r_i)} \right|. \quad (10)$$

3. RESULTS

For the resonators in the ground surface, validating laboratory measurement results are shown together with corresponding ones of using the model. Thereafter the model has been used to predict the performance of a strip of resonators alongside a two-lane road.

3.1 Comparison between calculations and laboratory measurements

A square grid of seven times seven resonators, with a centre-to-centre spacing of 30 mm, was placed with the openings in plane with an acoustically hard and smooth surface made of a surface-treated plywood. For the construction of the resonators, a 30 mm deep cavity with a grid of aluminium walls was manufactured together with a set of 2-mm-thick top aluminium plates with circular openings of different radii. The grid of resonators was placed in the centre of the 1.2x1.1 m² plywood plate. The measurements without effect of resonators were carried out by covering the openings by tape. A point source was simulated using a compression driver connected to a ca. 3 m long flexible hose with an aluminium ring at the opening, with an inner diameter of 25 mm. In Figure 3, these parts of the measurement setup are shown.

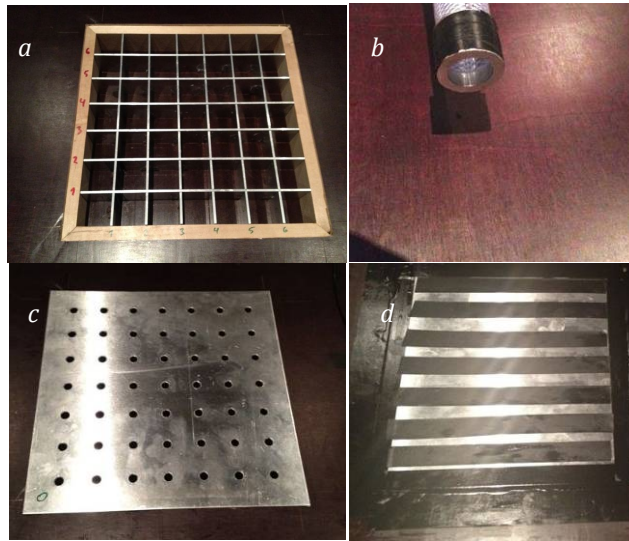


Figure 3 – Measurement setup for the grid of resonators: a) cavities, b) source, c) top plate, d) top plate openings covered by tape.

The sound source was placed at a height of 60 mm at a distance of 600 mm from the centre resonator along the centre line of the resonator grid. Feeding the loudspeaker with a white-noise signal the resulting sound pressure was measured using a quarter inch microphone (Larson Davis 2520, amplified using a G.R.A.S. Power Module Type 12AA). For each result, 30 averages of 0.4 s long signals were used.

Six different top plates were used to study the effect of varying the opening sizes, as shown in Table 1. Plates nr 5 and 6 are placed so that the opening radius is increasing row-wise from source toward microphone.

Table 1 – Variation of top plates with different resonator opening radii and corresponding resonance frequencies.

Top plate nr	Opening diameters	Estimated resonance frequency
1	all 6.0 mm	780 [Hz]
2	all 7.0 mm	862 [Hz]
3	all 8.0 mm	940 [Hz]
4	all 10.0 mm	1084 [Hz]
5	2.0, 3.0, 4.0, 5.0, 6.0, 7.0 and 8.0 mm	500–940 [Hz]
6	5.0, 5.5, 6.0, 6.5, 7.0, 7.5 and 8.0 mm	689–940 [Hz]

The various results are displayed in Figures 4–8. Unless otherwise stated, the receiver is placed on the plywood plate, 30 mm behind the last row of resonator openings and on-axis, i.e. so that the source–receiver line coincides with the centre line of the resonator grid. First it can be seen that there is good overall agreement between modelled and measured results. The agreement for plates nr 1–4 is very good, except slight deviation in resonance frequency as well as some disturbances that are most pronounced at higher frequencies (Figures 4 & 5). Similar disturbances were found in all measurements and may be due to waves from the resonators that are diffracted at the edge of the plywood plate.

Concerning the performance of the resonators, the insertion loss increases with opening area, as expected, i.e. from plate 1 to plate 4. As also expected, it can be seen that the noise reduction takes place from above the resonance frequency, extending in a tail toward higher frequencies, i.e. governed by the mass-behaviour of the resonators. The plates with mixed openings perform less well, i.e. plates 5 and 6 (Figure 6). Finally, the last three plots show that the model works also for other receiver positions: at a further distance behind the grid of resonators (Figure 7, left), off the central axis (Figure 7, right) and for an elevated receiver (Figure 8). Here, however, the disturbances become relatively larger, and the results show slightly less good agreement.

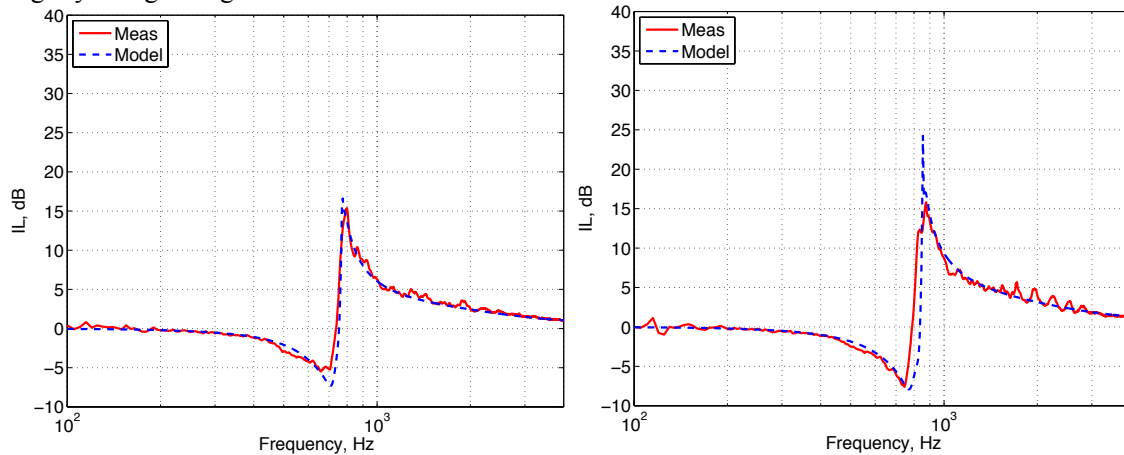


Figure 4 – Results for top plate nr. 1 (left) and top plate nr. 2 (right).

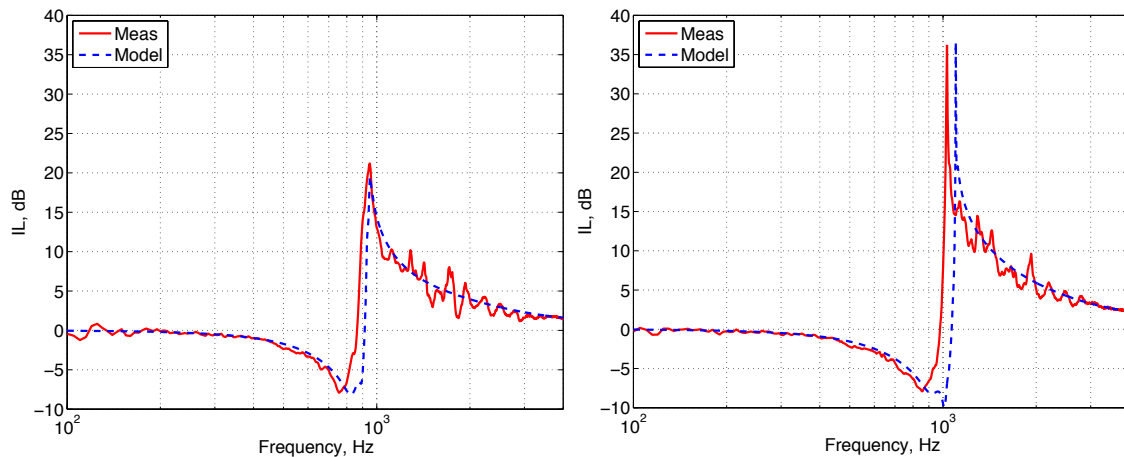


Figure 5 – Results for top plate nr. 3 (left) and top plate nr. 4 (right).

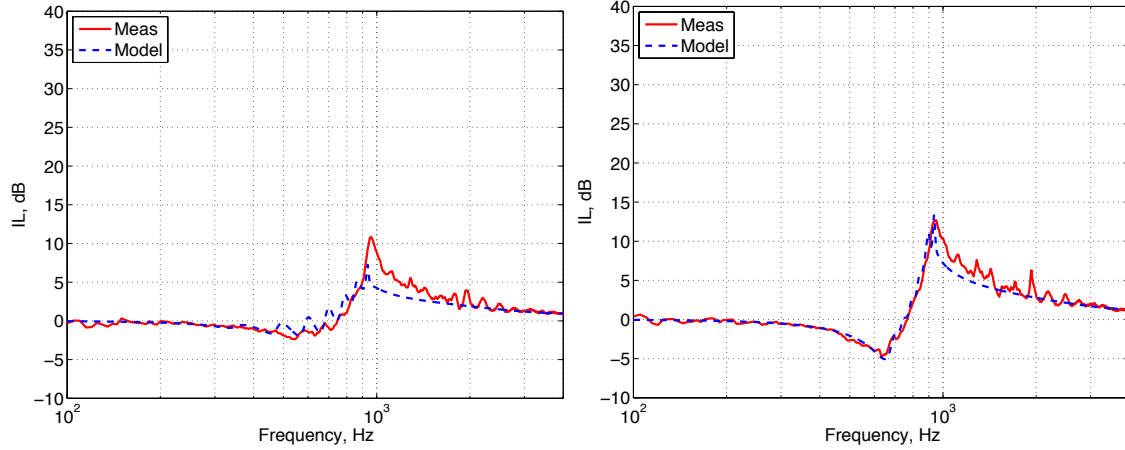


Figure 6 – Results for top plate nr. 5 (left) and top plate nr. 6 (right).

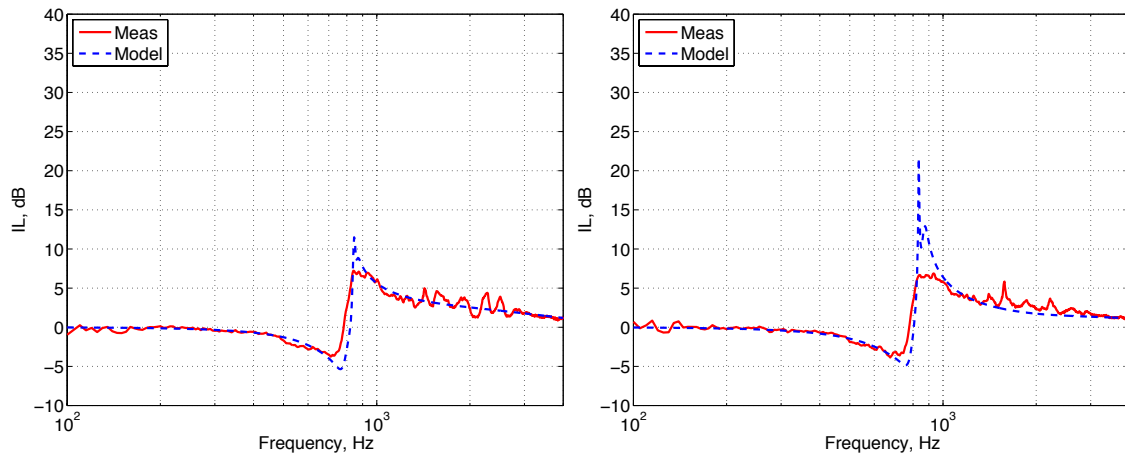


Figure 7 – Results for top plate nr. 2, with receiver 100 mm behind last row of resonator openings; on axis (left) and 90 mm off-axis (right).

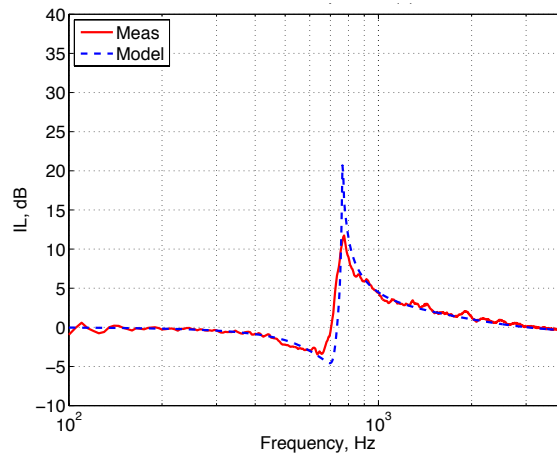


Figure 8 – Results for top plate nr. 1, receiver elevated to 60 mm.

3.2 Resulting insertion loss for a modelled grid of receivers along a road

Situations with a two-lane road are here used to give an estimate of the effect of roadside resonators. Each lane is modelled by sources at three heights according to the Harmonoise model for light and heavy-duty vehicles [3]: 0.01 m for rolling noise of both vehicle types; 0.3 m for light vehicle engine noise; and 0.75 m for heavy-duty vehicle engine noise. Also the source power spectra follow the Harmonoise model, including the partial power redistribution between rolling noise and engine noise. The horizontal

separation distance between the two lanes is 3.5 m, and the noise sources are modelled as being in the centre of a lane. At a horizontal distance of 2.5 m from the centre of one lane, a 4-m-wide strip of ground surface is devoted to resonators, in an otherwise hard ground. Using the numerical model, the effect of a square grid of resonators with 6 cm spacing is estimated. The resonators all have a resonance frequency of about 380 Hz and a circular opening with 20 mm diameter. The frequency region for expected noise abatement is hence above 380 Hz, which is targeting the source-spectrum peak region around 1 kHz. The plotted results are for 95 % passenger cars and 5 % trucks or buses (i.e. heavy-duty vehicles) at driving speeds of 50 and 70 km/h, as well as for only passenger cars at a driving speed of 50 km/h. For simplicity, a constant flow of 27,500 vehicles per day has been assumed for all three cases.

In Figures 9–11, the calculated sound pressure level is shown, with and without the resonators, for the third-octave bands 50–5000 Hz, and for a 1.5 m high receiver at 50 m range. As expected, the performance is better at higher frequencies, here, above 250 Hz. Below that frequency there is an estimated noise increase. In general, it is seen that the abatement using a 4-m-wide strip of resonators is calculated to give 2–4 dBA noise reduction for the various traffic cases. In specific, for 5 % heavy vehicles, the 70 km/h case is predicted to give slightly higher insertion loss than the 50 km/h case, about 3 dBA instead of 2 dBA, which is due to the relative increase in rolling noise at higher driving speeds, whereas for passenger cars only, at 50 km/h, the predicted insertion loss is about 4 dBA, which is due to the omission of the higher position engine source of the heavy vehicles.

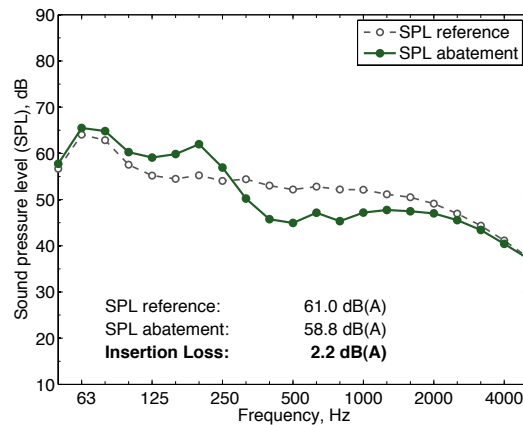


Figure 9 – Calculated sound pressure levels (SPL), with and without resonators, at 50 m range:
Driving speed 50 km/h, 5 % heavy vehicles.

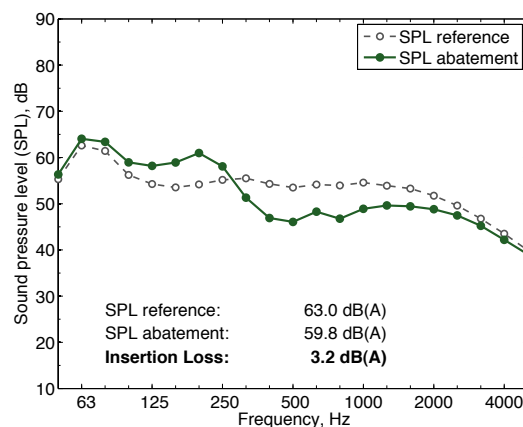


Figure 10 – Calculated sound pressure levels (SPL), with and without resonators, at 50 m range:
Driving speed 70 km/h, 5 % heavy vehicles.

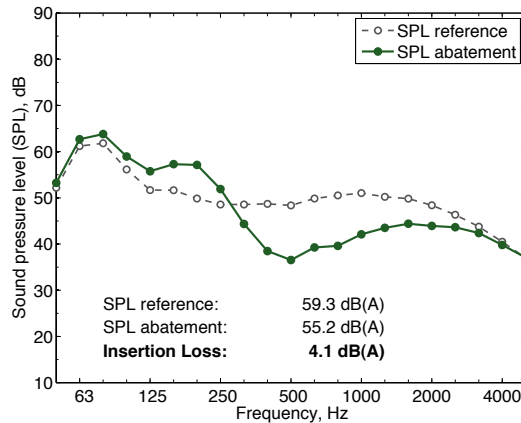


Figure 11 – Calculated sound pressure levels (SPL), with and without resonators, at 50 m range:
Driving speed 50 km/h, passenger cars only.

4. CONCLUSIONS

For roadside resonators of Helmholtz type, a numerical model has been developed and validated by laboratory measurements. The model has been used to estimate the effect of a 4-m-wide strip of resonators buried in the ground surface, using a centre-to-centre spacing of 6 cm, circular openings with 20 mm diameter and a common resonance frequency of about 380 Hz. Calculated sound pressure levels in the range 50–5000 Hz, with and without the resonators in an otherwise hard ground, show, for two-lane road traffic cases, estimated noise reductions of 2–4 dBA. There is also an estimated noise increase at lower frequencies, at 250 Hz and below.

Concerning further work, initial calculations show interesting results when raising a finite impedance strip to a moderate height of 0.3 m, whereby this is planned to be investigated further for the resonators. In addition, it would be of interest to reduce the predicted noise increase at lower frequencies. Furthermore, slightly higher insertion losses are expected if the strip is placed closer to the road track, which should be possible in practice since the resonators can be free from protruding elements.

ACKNOWLEDGEMENT

The research leading to these results has received funding from the European Community's Seventh Framework Programme (FP7/2007-2013) under grant agreement n° 234306, collaborative project HOSANNA.

REFERENCES

- [1] Ingard, U. On the theory and design of acoustic resonators. *Journal of the acoustical society of America*, Vol. 25, No. 6: 1037–1327, 1953.
- [2] Panton, R.L. and Miller, J.M. Resonant frequencies of cylindrical Helmholtz resonators. *Journal of the Acoustical Society of America*, Vol. 57, No. 6, Part II: 1533–1535 (1975).
- [3] Nota, R., Barelds, R. and van Maercke, D. Engineering method for road traffic and railway noise after validation and fine-tuning. Technical Report HAR32TR-040922-DGMR20 2005.